MM Science Journal | www.mmscience.eu
ISSN 1803-1269 (Print) | ISSN 1805-0476 (On-line)
Special Issue | HSM 2025
18th International Conference on High Speed Machining
October 15-16, 2025, Metz, France
DOI: 10.17973/MMSJ.2025_12_2025170

HSM2025-45080

A HYBRID APPROACH FOR OPTIMAL AND COMPACT DESIGN OF A COST-EFFECTIVE MAGNETIC ACTUATOR FOR INDUSTRIAL APPLICATIONS

Rakesh Verma[1], D.S. Srinivasu[*1]

[1]Indian Institute of Technology Madras, Department of Mechanical Engineering, Chennai, India

*Communicating Author, E-mail - devadula@iitm.ac.in

Abstract
Cutting tools with high length-to-diameter ratios used in internal turning often experience chatter due to increased compliance. To ensure stable machining, active damping methods using hydraulic-, piezoelectric-, magneto-strictive-, electromagnetic- actuators are explored earlier. Magnetic actuators stand out for their cost-effectiveness, manufacturability, and wide bandwidth. However, their bulky design limits industrial adaptability. This work proposes a hybrid approach that integrates numerical simulation with optimization to design compact and optimal magnetic actuators without sacrificing force/torque. The proposed approach resulted in an actuator having equivalent performance, enhancing suitability with dimensional reduction of (65.59%, 64.60%) for (Si-Fe, Ni-Fe) against Somaloy reported in literature.

Keywords:
Magnetic actuator, Chatter, Genetic algorithm

1 INTRODUCTION

Long and slender cutting tools are required to machine hollow and long cylindrical parts used in various automotive and aerospace applications. At high length-to-diameter (L/D) ratios, the cutting tools have high dynamic flexibility that produces self-induced vibrations known as chatter. Chatter results in poor surface finish, reduced material removal rate and low productivity that must be suppressed to improve productivity, which can be realized by incorporating either passive or active damping mechanisms in the cutting tools [Quintana 2011]. However, passive damped tools work for low frequencies and are effective only in the first mode. In addition, tuning the passive damped cutting tools is extremely challenging in practice [Fallah 2017]. On the other hand, the active-damped cutting tool has a high working bandwidth and can dampen multiple modes. An active damping mechanism is enabled by collectively using an actuator, an amplifier and a control mechanism. Different actuators, such as hydraulic [Glaser 1978], piezoelectric [Tewani 1995], magneto-strictive [Pratt 2001], and magnetic actuators [Lu 2014; Astarloa 2024], are one of the promising solutions. The actuators are intrinsically or extrinsically positioned in different boring bar assembly designs. Although the size of piezoelectric actuators is small, they are generally placed inside a cavity made in the cutting tool, which limits their force-exerting capability. In addition, the static stiffness of the cutting tool is compromised/reduced due to the cavity made for the placement of the actuator. Hydraulic, magnetostrictive actuators are large in size and attached externally to the cutting tools, thereby reducing the effective achievable L/D ratio. Magnetic actuators offer a cost-effective solution, are simple to produce, and operate over a wide bandwidth. Various electromagnetic actuators have been designed and used internally as well as externally. The internal placement of the actuator [Astarloa 2024; Abele 2016] is possible for high-diameter cutting tools (60 mm- 100 mm). However, magnetic actuators with components made of Somaloy [Lu 2014] are bulkier and mounted externally for cutting tools with low diameters (25 mm- 60 mm), which limits their industrial application. The size of the actuator is affected by the choice of material used in its fabrication. Therefore, obtaining an optimal actuator with a compact design with cost-effective material and ensuring its manufacturability is essential. In this context, the present study proposes a hybrid approach, which includes numerical simulations and evolutionary optimization to design a feasible and optimized magnetic actuator for real-time industrial applications. In the following *section 2* presents the scope of the present study, and *section 3* highlights the hybrid approach for optimization of a magnetic actuator design. *Section 4* discusses the demonstration of the proposed hybrid methodology. Results and discussions are presented in *section 5.* Finally, *Section 6* presents the summary of the current study.

2 SCOPE OF THE PRESENT STUDY

The current study proposes a hybrid approach to realize a compact and optimal design of the magnetic actuator by considering relatively high permeability and cost-effective materials compared to earlier materials. The proposed approach evaluates the force generated by the magnetic actuator using finite element (FE) model. The proposed hybrid approach that employs the FE model and

evolutionary optimization explores the optimal design. The critical steps involved in the proposed work are,

- To develop an FE model for the magnetic actuator to evaluate the force produced for a given design.
- To define the objective function for obtaining an optimized magnetic actuator design for the target force.
- To identify a high-permeability and cost-effective material that makes the magnetic actuator compact and cost-effective.
- To devise a hybrid framework that integrates FE model and optimization approach to identify the compact and optimal design.
- To demonstrate the proposed hybrid approach for its effectiveness.
- To establish a hypothesis testing framework to evaluate the statistical significance of the obtained optimized and compact design.

3 HYBRID APPROACH TO REALIZE A COMPACT AND OPTIMIZED DESIGN OF THE MAGNETIC ACTUATOR

Figure 1 presents the methodology employed to realize the compact and optimal design of a magnetic actuator, by the proposed hybrid approach that makes it adaptable to the industry in terms of practicality/employability and cost effectiveness. The methodology comprises of (i) development of the FE model of the magnetic actuator for the evaluation of the force generated, and (ii) integrating the evolutionary optimization algorithm with the FE model by defining a practical objective function. Finally, a hypothesis testing framework is proposed to evaluate the significance of the results provided by the proposed hybrid approach. The above steps are detailed in the following subsections.

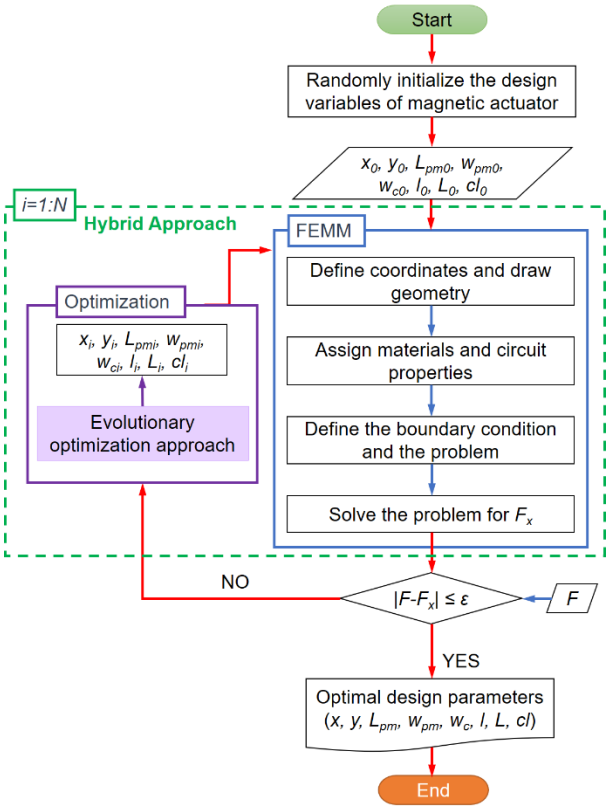

Fig.1: Flowchart for the magnetic actuator design optimization

3.1 FEM modelling

Magnetic actuators are typically designed according to specific application requirements and consist of key components such as stator, rotor, permanent magnets (PMs), coils, *etc*. Design parameters are primarily dictated by the geometry of each component, which includes (a) dimensions of the stator and rotor, (b) the size and placement of permanent magnets, and (c) coil dimensions and wire gauge. The aim towards developing the FE model of the magnetic actuator is to predict the force/torque for a given set of design parameters. Towards developing the FE model, the following steps have been followed:

Step 1: The relevant design variables, such as air gaps (x, y), dimensions of the stator, armature (L, l), permanent magnets (l_{pm}, w_{pm}), coil size (w_c), and clearances (cl), *etc.*, were identified and defined to develop the actuator's geometry through coordinate specification in the FEM model.

Step 2: The materials were selected as Si-Fe or Ni-Fe and assigned to the components made of soft magnetic materials by considering the non-linear B-H relationship. For permanent magnets, the magnetisation direction was defined in addition to the non-linear B-H relationship.

Step 3: A suitable coil wire gauge was selected according to the current requirement, and allocated to the coil regions, followed by the definition and assignment of circuit properties, where the current supplied is specified.

Step 4: A Dirichlet boundary condition was applied, and the magnetostatics problem was configured. After mesh generation, the simulation was run to compute the magnetic field and determine the resulting force generated by the actuator.

3.2 Evolutionary optimization approach

A family of algorithms motivated by the principles of natural evolution to solve complex optimization problems are known as evolutionary algorithms (EAs). These operate by generating a population of probable solutions over successive generations, directed by a fitness function that evaluates the quality of the solution. The following steps were taken to implement the evolutionary optimization approach:

Step 1: A suitable range of the magnetic actuator design variables, such as air gaps (x, y), dimensions of the stator, armature (L, l), permanent magnets (l_{pm}, w_{pm}), coil size (w_c), and clearances (cl), *etc.*, was defined according to the design requirements.

Step 2: Among various evolutionary algorithms, the genetic algorithm (GA) was selected for optimization due to its high reliability, capability to find the global optimum region, and a clearly defined objective function and constraints to drive the optimization process.

Step 3: The optimization process was started by randomly initializing the design variables, which were then input into FE model for simulation.

Step 4: The output from the FE model was then used to evaluate the objective function $||F_x| - F| \leq \varepsilon$. Here, F_x is the force obtained from the FE model, F is the desired magnitude of force defined by the user, and ε is the extremely small value specified by the user.

Step 5: If the optimization criterion is satisfied, the process concludes, and the optimal design parameters were determined.

Step 6: If not, the algorithm generates a new set of variables within the predefined range, and steps 3 and 4 will be repeated until convergence is achieved.

3.3 Statistical Hypothesis-Testing Framework

The proposed hybrid optimization may yield configurations that can appear superior in compactness or efficiency. However, due to variability in optimization outcomes and inherent uncertainties in design parameters, assessing whether such improvements are statistically reliable is essential. Hypothesis testing provides a rigorous framework for distinguishing accurate material- or design-driven effects from differences that could arise by chance.

This study employs hypothesis testing to formally evaluate whether optimized actuators with Si-Fe and Ni-Fe parts achieve statistically significant reductions in selected endpoints compared to the Somaloy reference design. Additionally, it enables a direct comparison between the two optimized material systems. The main goal is to verify that the observed improvements in compactness are not artefacts of numerical variability, but instead represent reproducible and meaningful gains attributable to material choice.

The primary endpoint under consideration is the actuator footprint, expressed as the effective surface area, and the secondary endpoints are PM area and stator width. Statistical hypotheses were formulated to evaluate whether the optimized designs (Si–Fe and Ni–Fe) achieve significant improvements in footprint relative to the Somaloy reference, and to compare the two optimized material systems. Endpoint values were obtained by varying the materials of the actuator parts among three materials:

- **Somaloy reference:** Computed once from the reported literature geometry.
- **Optimized actuator with Si-Fe and Ni-Fe:** Ten optimal solutions were obtained through the hybrid design optimization procedure.

Hypotheses for Statistical comparisons were formulated as follows:

- **Si–Fe vs. Somaloy:**

$$H_0 : \mu_{Si-Fe} \geq \mu_{Somaloy},$$
$$H_1 : \mu_{Si-Fe} < \mu_{Somaloy}$$

(one-sided test: improvement corresponds to a smaller footprint, PM area and stator width).

- **Ni–Fe vs. Somaloy:**

$$H_0 : \mu_{Ni-Fe} \geq \mu_{Somaloy},$$
$$H_1 : \mu_{Ni-Fe} < \mu_{Somaloy}$$

(one-sided test: improvement corresponds to a smaller footprint, PM area and stator width).

- **Si–Fe vs. Ni–Fe:**

$$H_0 : \mu_{Si-Fe} = \mu_{Ni-Fe},$$
$$H_1 : \mu_{Si-Fe} \neq \mu_{Ni-Fe}$$

(Two-sided test: no differences in footprint, PM area, or stator width).

Where, H_0 and H_1 represents null and alternative hypotheses, respectively.

4 DEMONSTRATION OF THE PROPOSED APPROACH

To demonstrate the proposed methodology, a magnetic actuator [Lu 2014] designed for chatter suppression during internal turning is considered. *Subsection 4.1* discusses the design and configuration of the magnetic actuator and the principle of active damping. *Subsection 4.2* details the materials and the specific conditions considered for FE modelling and optimization.

4.1 Actuator Configuration and principle of active damping

Figure 2 shows the schematic of the magnetic actuator that consists of four stators, one armature and four permanent magnets. Two coils are wound around each stator. When the currents are supplied in the direction as shown in the top and bottom stator coils, the magnetic force is generated in the x-direction. Similarly, it can generate force in the y-direction when currents are supplied in the left and right stator coils. This actuator is capable of generating a torque when current is supplied to all the stator coils. The main design parameters of the actuator are length of PM (l_{pm}), width of PM (w_{pm}), air gap between stator and armature (x), air gap between armature and PM (y), width of coil (w_c), clearance between coil and PM (cl) and distances l and L. Figure 3(a) presents the schematic of active damped system, which consists of a stationary cutting tool, a hollow cylindrical rotating workpiece, an accelerometer, a data acquisition (DAQ) system, a controller, an amplifier and an actuator. The principle of active damping is to produce a counter vibration based on the vibration measured at the tip of the cutting tool to diminish the vibration at the tip, as shown in Fig. 3(b).

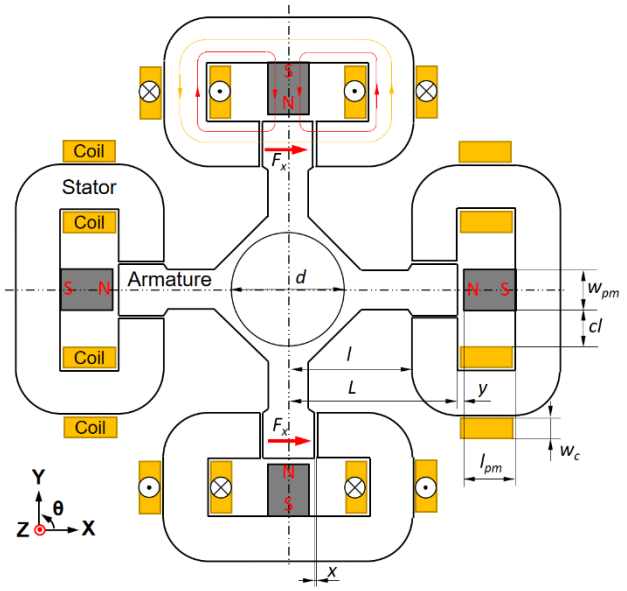

Fig. 2: Schematic of the considered magnetic actuator.

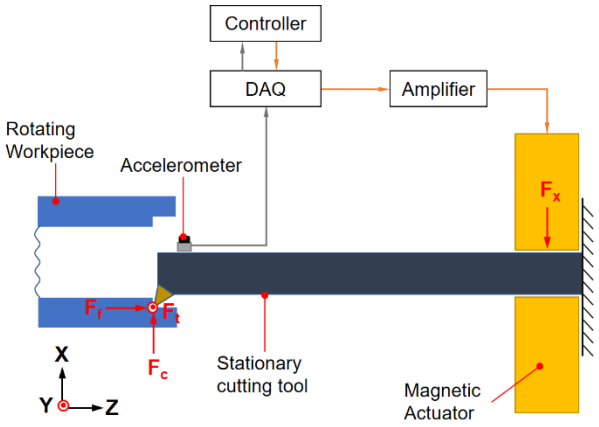

(a)

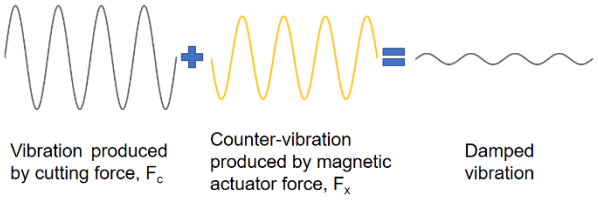

(b)

Fig. 3: Active damped system for internal turning: a) schematic, and b) principle

4.2 Considerations for FE modelling and GA Optimization

For further analysis, the stator and armature are assumed to be fabricated from laminated Si-Fe selected for their high permeability, cost-effectiveness and broad commercial availability, and Ni-Fe selected for high permeability, high saturation flux density, and very low core loss. The actuator employs a Neodymium magnet ($Nd_2Fe_{14}B$, Grade 42SH), a rare-earth material known for its superior magnetic properties. Coil windings around each stator are formed using solid bare copper wire, 20 AWG, with a diameter of 0.81 mm. The coil windings are maintained at a fixed count of 256 turns, with a constant supply current of 1 ampere. First, the considered actuator was modelled in FEMM and simulated to produce a force of 370 N. This modelled actuator is then subjected to an optimization process for two different stator and armature materials. The main objective of the optimization is to find optimal design parameters to get a compact actuator without any compromise with force-producing capability. The objective function is defined by Eq. (1) as,

Objective function:

$$Min\{F - F_x\} = f(L, l, w_{pm}, l_{pm}, x, y, w_c, cl) \quad (1)$$

Constraints: $L - l \geq 6;$

$$2l - w_c - cl - L - w_{pm}/2 - x \geq 0$$

$$(l_{pm} + y - 3) - w_c \geq 0$$

Here, F_x is the force acting on the armature evaluated from FEMM simulations. The magnetic force produced by the actuator is computed by the eggshell method [Henrotte 2004], considering Maxwell stress tensor theory as presented in Eq. (2):

$$F_x = \int_S \nabla\phi . \sigma \, dS \quad (2)$$

where, F_x is the magnetic force acting on the armature, σ is the Maxwell stress tensor, ϕ is the weighting function, and $\nabla\phi$ is the gradient of the weighting function.

The considered design variables with lower and upper bounds are listed in Table 1. The optimization process was performed in MATLAB® by randomly initializing the design variables, which were then provided to the FE model.

Tab. 1: Magnetic actuator design parameters

Design parameter (mm)	*L*	*l*	l_{pm}	w_{pm}	w_c	*cl*	*x*	*y*
Lower bound	40	25	7	7	4	4	0.5	2
Upper bound	60	45	20	20	8	8	1	5

5 RESULTS AND DISCUSSIONS

Actuator parts (stator and armature) were assigned two different materials, *i.e.,* Si-Fe and Ni-Fe, and compared with Somaloy. Optimizations were repeated 10 times for Si-Fe and Ni-Fe by considering all the defined design parameters of the magnetic actuator. The actuator's thickness was maintained constant at 48 mm throughout the optimisation process.

5.1 Optimal design parameters

The mean and standard error from the observed set of optimal design parameters were evaluated as given by Eq. (3):

$$SE = \frac{s}{\sqrt{n}} \quad (3)$$

where, *s* is the sample standard deviation and *n* is the sample size for the design parameters.

Figure 4 presents the bar graph that compares the design parameters for three different materials: Somaloy [Lu 2014], Si-Fe, and Ni-Fe. The y-axis represents the dimension of the design parameter with its standard error in millimetres (mm), and the x-axis lists the stator and armature material.

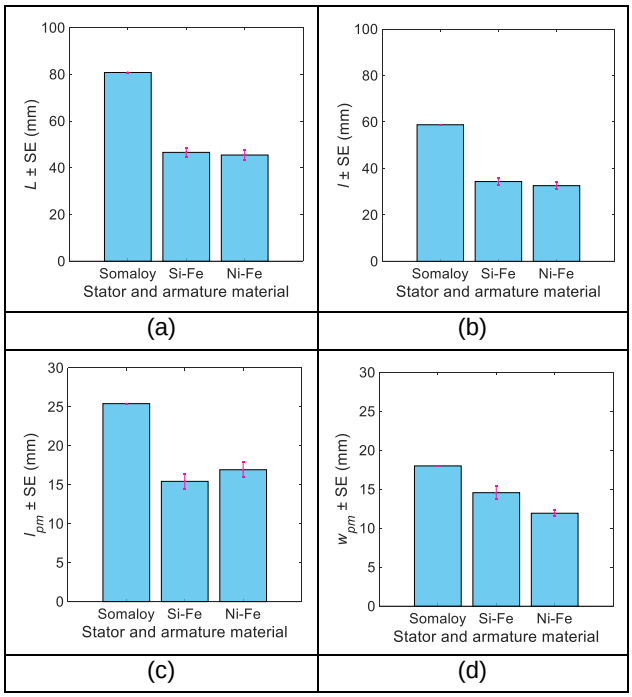

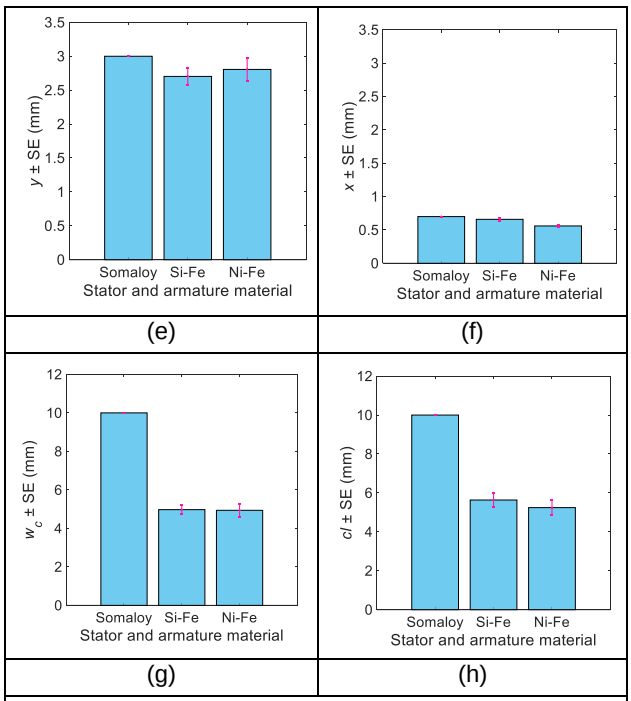

Fig. 4: Optimal design parameters for different stator and armature materials, (a) L, (b) l, (c) l_{pm}, (d) w_{pm}, (e) x, (f) y, (g) w_c, and (f) cl

The design parameters tend to have similar values for Si-Fe and Ni-Fe. The error bars were relatively minor for most parameters, suggesting high precision or low variability, except for *L* and *l*, where the error bars are larger. For all materials, negligible variation was observed in the air gap between the stator and armature (*x*), and the air gap between the armature and the permanent magnet (*y*). A reduction of 42.33% and 43.73% was observed for the design parameter (*L*) in the case of Si-Fe and Ni-Fe as compared to Somaloy. The design parameter (*l*) was reduced by 41.58% and 44.60% for Si-Fe and Ni-Fe compared to Somaloy. Furthermore, the width of the stator is dictated by '*L-l*', which got reduced from 22 mm for Somaloy to 12.24 mm, *i.e.,* 44.36% reduction for Si-Fe and 12.89 mm, *i.e.,* 41.44% reduction for Ni-Fe. In comparison to Somaloy, a significant decrease in the dimension of the permanent magnets (*i.e.,* l_{pm} × w_{pm}) was achieved, from 25.4 × 18 mm^2 for Somaloy to 15.42× 14.56 mm^2, *i.e.,* 50.89% reduction for Si-Fe and 16.91 × 11.92 mm3, *i.e.,* 55.91% reduction for Ni-Fe. The surface area occupied by the magnetic actuator was 262.4 × 262.4 mm² for Somaloy, 153.92 × 153.92 mm² for Si-Fe and 156.12 × 156.12 mm² for Ni-Fe. Consequently, the surface area of the optimized actuator was reduced by 65.59% for Si-Fe and 64.60% for Ni-Fe, respectively. The optimal design parameters of the magnetic actuator for Si-Fe and Ni-Fe stator and armature are listed in Tables 2 and 3. The reduction in the actuator footprint can be attributed to high permeability, high saturation flux density, and very low core loss in the case of Si-Fe and Ni-Fe.

Therefore, the hybrid optimization approach demonstrates that the redesigned actuator achieves a more compact footprint while maintaining high performance and output generation. Furthermore, two sets of optimizations were repeated 10 times for Si-Fe and Ni-Fe each by considering different ranges of all the defined design parameters of the magnetic actuator. It was observed that the overall reduction in the footprint of the magnetic actuator was the same in both sets of the optimization, ensuring repeatability. Additionally, hypothesis test results are presented in the following subsection to evaluate the statistical significance of the obtained parameters.

Tab. 2: Optimal design parameters of the magnetic actuator for Si-Fe stator and armature

Design parameter (mm)	***L***	***l***	l_{pm}	w_{pm}	w_c	***cl***	***x***	***y***
Mean	46.59	34.35	15.42	14.56	4.97	5.63	0.65	2.7
Standard error	1.82	1.66	0.93	0.86	0.25	0.35	0.02	0.12
Confidence level (95%)	4.11	3.77	2.12	1.95	0.56	0.8	0.05	0.28

Tab. 3: Optimal design parameters of the magnetic actuator for Ni-Fe stator and armature

Design parameter (mm)	***L***	***l***	l_{pm}	w_{pm}	w_c	***cl***	***x***	***y***
Mean	45.46	32.57	16.91	11.92	4.93	5.24	0.56	2.8
Standard error (SE)	2.1	1.52	0.94	0.37	0.34	0.38	0.01	0.17
Confidence level (95%)	4.75	3.44	2.13	0.85	0.78	0.86	0.03	0.38

5.2 Hypothesis test results

A comprehensive statistical analysis of footprint areas achieved through genetic algorithm (GA) optimization for two core materials: Silicon-Iron (Si-Fe) and Nickel-Iron (Ni-Fe) alloys, was compared against a Somaloy reference material. The analysis was carried out on the actuator's footprint area, PM area and stator width obtained for three core materials:

- **Si-Fe alloy**: n = 10 samples
- **Ni-Fe alloy**: n = 10 samples
- **Somaloy reference**:
  μ_0 (Footprint area) = 68,853.76 mm²
  μ_0 (PM area) = 472.2 mm²
  μ_0 (Stator width) = 22 mm

Before proceeding to hypothesis testing, data normality was evaluated using the Lilliefors test. The normality assumptions were verified for both materials. For testing the hypotheses formulated in section 3.3, three comparisons for primary and secondary endpoints were conducted:

1. One-sample t-tests for comparing each material against the Somaloy reference.
2. Two-sample Welch's t-test for comparing Si-Fe and Ni-Fe means

Furthermore, the effect size was calculated by computing Cohen's d for all comparisons and applying it to the two-sample comparison. All analyses were conducted in MATLAB® with a significance factor (α = 0.05). The comparative statistical evaluation confirms the strong

influence of genetic algorithm (GA)-based optimization on reducing core footprint and associated design parameters. For the **Si-Fe vs Somaloy** comparison, the one-sample t-test revealed a significant reduction in footprint area ($p = 7.94 \times 10^{-11}$), with Cohen's d = -9.97 indicating a considerable effect size. This result rejects the null hypothesis, confirming that the reduction is statistically significant and practically meaningful. Similar reductions were observed in the PM area and stator width, demonstrating the consistency of the GA optimization across multiple design variables.

A comparable outcome was obtained in the **Ni-Fe vs Somaloy** analysis. The one-sample t-test reported a significant reduction in footprint area ($p = 1.87 \times 10^{-10}$), accompanied by a large effect size (Cohen's d = -9.06). As with Si-Fe, reductions in PM area and stator width were also evident, confirming that Ni-Fe benefits substantially from GA optimization.

When **Si-Fe and Ni-Fe** were directly compared, the Welch's two-sample t-test showed no statistically significant difference in their optimized footprint areas ($p = 0.739$). The trivial effect size (Cohen's d = -0.152) supports the conclusion that both alloys respond equivalently to GA-based optimization. Thus, the null hypothesis of no difference between Si-Fe and Ni-Fe cannot be rejected.

The magnitude of the improvements achieved under GA optimization is of particular engineering relevance. Si-Fe and Ni-Fe demonstrated ~65–66% footprint reductions compared to the Somaloy reference, with very large effect sizes (Cohen's d > 6). These results extend beyond statistical significance to highlight the practical importance of the optimization strategy.

These findings have important implications for the design and optimization of magnetic cores. The equivalence in performance between Si-Fe and Ni-Fe under GA optimization indicates that the choice of alloy can be guided by practical engineering considerations—such as raw material cost, availability, processing characteristics, and manufacturing constraints—rather than by optimization outcomes. This flexibility enhances the applicability of GA optimization in real-world design scenarios, where non-performance factors often play a critical role in material selection.

Moreover, the consistency of improvements across different materials demonstrates that GA optimization is a robust and material-agnostic strategy within this class of alloys. By enabling highly efficient gains in footprint and associated parameters, the GA-based approach offers a powerful tool for advancing magnetic core design. These results establish GA optimization as a technique for achieving superior performance and a scalable and generalizable framework that can be integrated into future design pipelines.

SUMMARY

The proposed hybrid approach for realizing a compact and optimal magnetic actuator is demonstrated towards making it more practical for industrial applications. For this purpose, the optimization method identified the optimal dimensions of the actuator through its explorative capabilities when integrated with the model based on finite element (FE) methodology that predicts the force for the given configuration of the magnetic actuator supplied by the optimization method.

From the results, it was observed that,

- The width of the stator decreased by 44.36% and 41.44% in the case of Si-Fe and Ni-Fe, respectively.
- A total reduction of 50.89% and 55.91% in the dimensions of permanent magnets was achieved in the case of Si-Fe and Ni-Fe stators and armatures, respectively, leading to a corresponding decrease in material cost.
- The actuator's footprint, in terms of surface area, was reduced to 65.59%for Si-Fe and 64.60% for Ni-Fe in comparison to Somaloy.
- The reduction obtained in the actuator's footprint area, permanent magnet area, and stator width is statistically and practically significant as demonstrated in the hypothesis tests.
- No significant differences were observed in the endpoints between Si-Fe and Ni-Fe.

Although the present work helped in identifying the optimal design parameters of the magnetic actuator, it does not account for the manufacturability constraints of the obtained optimal solutions. In addition, this study addresses the actuator's design and static force geometry optimization. Therefore, manufacturability and evaluation of the dynamic characteristics can be explored as a future scope in the context of active damping applications.

6 ACKNOWLEDGMENTS

The authors would like to acknowledge the support of IITM PRAVARTAK Technologies Foundation, funded by the Department of Science and Technology, Government of India, under the National Mission on Interdisciplinary Cyber-Physical Systems. The financial assistance provided for the project titled *'Development of IIoT-enabled Active Damped Boring Bar to Mitigate Chatter in Machining of Aerospace Alloys'* (Project No.: PRA/21–22/003/SIVA) was instrumental in carrying out this research work.

7 REFERENCES

[Quintana 2011] Quintana, G and Ciurana J. Chatter in machining processes: A review. International Journal of Machine Tools and Manufacture, 2011, Vol.51, No.2, pp 363–376. ISSN 08906955

[Fallah 2017] Fallah, M., and Moetakef-Imani, B. Analytical prediction of stability lobes for passively damped boring bars. Journal of Mechanics, Vol.33, No.5, pp 641-654. ISSN 18118216

[Glaser 1978] Glaser, DJ and Nachtigal, CL. Development of a hydraulic chambered, actively controlled boring bar. New York, US.a, Asme, December 1978, Vol.1, pp 362–368.

[Tewani 1995] Tewani, SG, et al. A study of cutting process stability of a boring bar with active dynamic absorber. International Journal of Machine Tools and Manufacture, Vol.35, No.1, pp 91–108. ISSN 08906955

[Pratt 2001] Pratt, J. R., and Nayfeh, A. H. Chatter control and stability analysis of a cantilever boring bar under regenerative cutting conditions. Philosophical Transactions of the Royal Society of London. Series A: Mathematical, Physical and Engineering Sciences, 2001, Vol.359, No.1781, pp 759-792. ISSN 1364503X

[Lu 2014] Lu, X, et al. Magnetic actuator for active damping of boring bars. CIRP Annals - Manufacturing Technology, Vol.63, No.1, pp 369–372. ISSN 17260604.

[Astarloa 2024] Astarloa, A, et al. Reluctance-Based Modular Active Damper for Chatter Suppression in Boring Bars With Different Overhangs. IEEE/ASME Transactions on Mechatronics, February 2024, Vol.29, No.1, pp 679–690. ISSN 1941014X

[Abele 2016] Abele, E. et al. Adaptronic approach for modular long projecting boring tools. CIRP Annals - Manufacturing Technology, 2016, Vol.65, No.1, pp 393-396. ISSN 17260604

[Henrotte 2004] Henrotte, F, et al. The eggshell approach for the computation of electromagnetic forces in 2D and 3D. COMPEL-The international journal for computation and mathematics in electrical and electronic engineering, Vol.23, No.4, pp 996-1005.